Review on processing stability, weld defects, finite element analysis, and field assisted welding of ultra-high-power laser (≥ 10 kW) welding

Lu Wang and Youmin Rong*

School of Mechanical Science and Engineering,
Huazhong University of Science and Technology,
Wuhan, China
Email: wl103002@163.com
Email: rym@hust.edu.cn
*Corresponding author

Abstract: The ultra-high-power laser welding, with obvious characteristics of fast welding speed, small heat input, small deformation, large aspect ratio, high alignment, and high directivity, has a huge application potential. In this paper, the research findings and progress for ultra-high-power laser welding are critically reviewed in the last ten years. The investigation state of ultra-high-power laser welding is classified and summarised from the point of processing stability, common weld defects, application of numerical simulation, and external field assisted welding. Finally, the potential research problems and challenges based on ultra-high-power laser (≥ 10 kW) welding are discussed. This fundamental work aims to review the research progress in laser welding monitoring and provide a basis for follow-on research.

Keywords: laser welding; ultra-high-power laser; processing; defects; numerical simulation; external field.

Reference to this paper should be made as follows: Wang, L. and Rong, Y. (2022) 'Review on processing stability, weld defects, finite element analysis, and field assisted welding of ultra-high-power laser (≥ 10 kW) welding', *Int. J. Hydromechatronics*, Vol. 5, No. 2, pp.167–190.

Biographical notes: Lu Wang received her BSc in Mechanical Engineering from the Northeastern University, Shenyang, China in 2019. She is currently studying for a PhD at the Huazhong University of Science and Technology. Her research interests are laser welding, thick plate welding, and simulation of welding residual stress.

Youmin Rong received his PhD from the School of Mechanical Science and Engineering, Huazhong University of Science and Technology (HUST), Wuhan, China in 2013 and 2017. He worked as a Lecturer in the School of Mechanical Science and Engineering of HUST from 2019 to 2020. He is currently an Associate Professor at the HUST. He has published 35 journal papers. His current research interests include laser manufacturing. From 2013 to 2017, he worked as an assistant with Wuhan Donghu University. His research interests include machine vision, vision-aided robotic welding, and weld seam tracking. He is a member of the Hubei Society of Mechanical and Electrical Engineering. He has published several papers in IEEE.

Copyright © 2022 Inderscience Enterprises Ltd.

1 Introduction

Light amplification by stimulated emission of radiation (laser) is one of the greatest inventions in the 20th century. With outstanding advantages of good monochrome, high brightness, and good direction, the laser has been widely used in industry, medicine, commerce, scientific research, information, and military. Through retrieval and analysis in Web of Science (topic: laser, timespan: 2015–2019), the number of literatures is 477,992, and its related engineering accounts for 61.48%. The investigation of engineering-oriented laser applications is very active, especially in laser manufacturing (Laser manufacturing accounts for 37.65% in engineering-oriented laser applications).

Laser manufacturing methods mainly consist of welding, cutting, cladding, shocking, marking, drilling, heat treatment, additive manufacturing, etc. Under the same retrieval condition as above, the research tendentiousness of different laser manufacturing is analysed. Laser welding attracts the attention of many researchers, and its proportion (23%) is a quarter of the total. Twenty years ago, ultra-high-power laser (≥10 kW level, UHPL) was used to weld metal material (Ito et al., 1999), and a single-pass penetration of 70 mm was obtained by 100 kW fibre laser (Kawahito et al., 2018). With higher power, operation stability improvement, and cost reduction, applying UHPL has become popular to advance manufacturing, especially for laser welding. However, UHPL welding focuses on metal welding, while non-metal welding (or joining) currently adopts low-power (≤100 W) laser welding. There are many problems in UHPL welding of non-metallic material owing to material properties [for inorganic non-metallic materials such as glass and ceramics, powerful continuous-wave lasers without high-temperature preheating have been unsuccessful because of macroscopic cracking attributed to thermal shock (Penilla et al., 2019)], energy requirements (melting requires much less energy than metal), and so on.

Ultra-high-power laser welding, with obvious characteristics of fast welding speed, small heat input, small deformation, large aspect ratio, high alignment, and high directivity, has a huge application potential. In this paper, an overview of UHPL welding was arranged in detail, which can be divided into four important parts. In the first part (Section 2), the processing stability of UHPL welding is summarised. The morphological characteristics and dynamic behaviour of keyhole, weld pool, and plume have been analysed, while the mechanical properties of weld joints have been introduced. In the second part (Section 3), the formation mechanism and control methods of weld defects were sorted and summarised, respectively. In the third part (Section 4), several numerical simulation methods are reviewed according to different prediction targets such as keyhole and weld pool simulation, welding residual stress simulation, and phase change process simulation. In the fourth part (Section 5), the optimisation of different external fields on UHPL welding are classified and summarised. The relationship between the four parts is shown in Figure 1. A stable welding process is the key to obtain a weld joint with good performance and no weld defects. The simulation is used to obtain the variation of the physical quantity which can not be easily observed in the experiment, shorten the experiment time, and reduce the experiment cost. Field assisted welding is an effective measurement to stabilise welding process and reduce welding defects. At the end of the article, the potential future research work and challenges about UHPL welding were discussed. This paper aims to provide a basis for follow-on research by reviewing the research trends in the past ten years.

Figure 1 The review structure and the relationship of each chapter of this paper (see online version for colours)

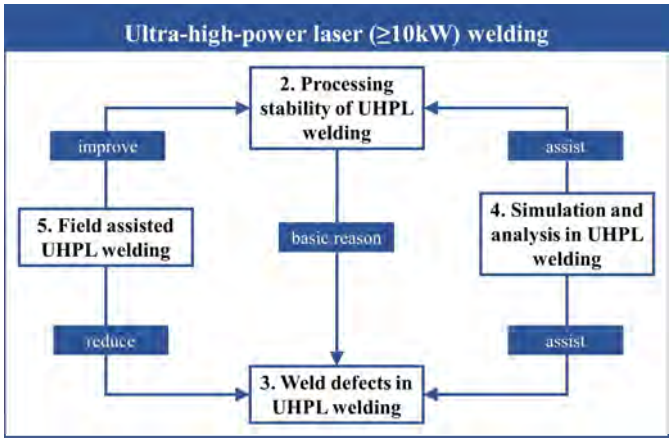

2 Processing stability of UHPL welding

In the process of UHPL welding, the laser beam with ultra-high-power density has an intense interaction with the material, and the dynamic behaviours of keyhole, weld pool, and plume are intense. Therefore, the welding process stability is poor, which greatly affects the weld morphology and performance. Many researchers have studied the processing stability of UHPL welding from the view of keyhole, weld pool, plume, and joint performance. The morphological characteristics and dynamic behaviour of keyhole, weld pool, and plume have been analysed, while the mechanical properties of weld joints have been investigated. In addition, keyhole, weld pool, plasma, and other optical and spectrum information of the welding can be used to online monitor the welding statuses (Chen et al., 2018b; Zhang et al., 2019b). As the research content is more related to signal acquisition, program design, etc. it is not described in detail in this paper.

The keyhole is the phenomenon of vapour depressions during laser melting of metals, which is an important characteristic of UHPL welding. The X-rays method is used by Kawahito et al. (2009) to observe the dynamic behaviour of keyhole. To more clearly distinguish the interface wall between keyhole and weld pool, Zhang et al. (2013a) proposed a modified 'sandwich' specimen method to directly observe the keyhole dynamic behaviour in laser welding. With the help of a high-speed camera, the keyhole wall and weld pool flow (Figure 2) can be clearly captured. It can be found that the wall of keyhole is constantly fluctuating during the welding process. The flow of metal vapour in the keyhole (Li et al., 2014a) and liquid metal outside the keyhole (Fabbro et al., 2006) are the key factors of keyhole oscillation. In addition, Zhang et al. (2019b) found that the keyhole width reached the quasi-steady state earlier than the keyhole depth. In other words, higher laser power results in a more unstable keyhole. The oscillation of keyhole will reduce the stability of welding process and thus affect the quality of the weld formation. The laser optical system with long focus depth (Matsumoto et al., 2017), welding assisted with external gas jet (Xing et al., 2017), and nitrogen shielding gas (Kawahito et al., 2009) both can improve the keyhole stability.

Figure 2 Application of a modified sandwich specimen to observe the longitudinal keyhole during 10 kW fibre laser welding (see online version for colours)

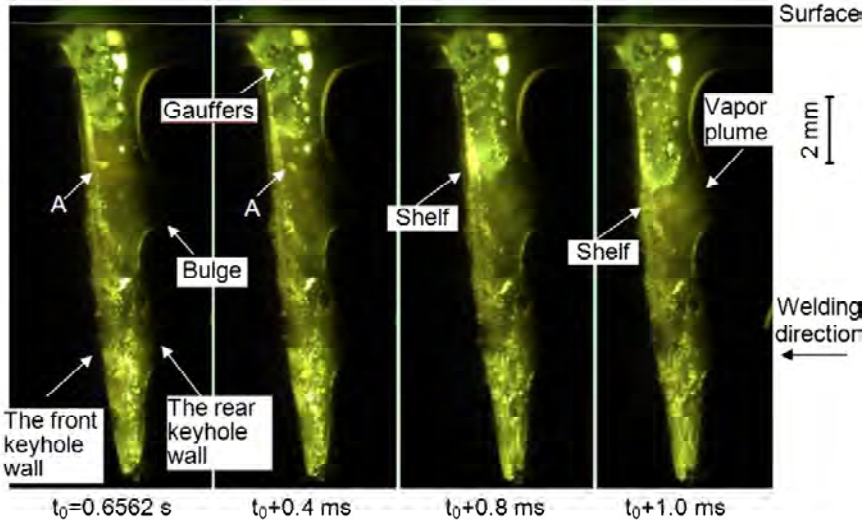

Note: Welding speed 1.2 m/min, defocus length 5 mm.

Source: Zhang et al. (2013a, p.20001)

The weld pool is the part of the base metal that is heated by the laser and melted, which is the liquid metal around the keyhole. In UHPL welding, driven by complex driving forces, such as vapour pressure, surface tension, etc. the flow of weld pool is intensified, and the weld formation will be directly affected (Fabbro, 2010; Ai et al., 2021). There are two common means of weld pool observation: heterogeneous element labelling and the 'sandwich method' combined with a high-speed camera. The distribution and flow trend of weld pool can be captured by tracing the trajectories of some added special particles (Kawahito et al., 2009; Li et al., 2014b). A butt configuration of metal and transparent quartz glass also can be used to observe the weld pool geometry through a high-speed camera and an infrared camera recording. Zhang et al. (2016) studied a lower-cost method to obtain weld pool morphology. The welding stick with dissimilar elements was placed at the end of welding, a dissimilar metal is introduced into the weld pool. The shape of the region of the weld that contains the dissimilar elements can be approximately considered to be the shape of the weld pool.

The plasma is the gasification product of base metal caused by laser energy input. Plasma resides both outside and inside the keyhole, known as plasma plume and keyhole plasma, respectively. The eruption of plasma in UHPL welding is more violent than that in low-medium power laser welding, and this phenomenon has a negative influence on process stability (Li et al., 2015a). First, the weld penetration in CO_2 laser welding will be drastically reduced by the oscillation of plasma (Beyer et al., 1984). However, the ionisation of fibre laser is weaker than that of CO_2 laser, the effect of plasma on the penetration depth is small in fibre welding (Kawahito et al., 2008a, 2008b; Bykovskiy et al., 2015). Secondly, the plasma affects the generation, speed, and volume of the spatter. With the absorption and uneven distribution of energy in the keyhole and near zone (Li et al., 2014b), the high-temperature plasma is ejected by a large recoil pressure, and some liquid metal is taken out to form the spatter (Li et al., 2014c). The accelerated

speed and increased volume of spatter are affected by the plasma (Kaplan et al., 2008). The fluctuation of keyhole is the main source for the oscillation of the plasma (Li et al., 2015a; Wang et al., 2012). In other words, the stability of welding process is mainly affected by the keyhole plasma. Therefore, increasing the stability of the keyhole is positive to reduce the plasma instability.

Figure 3 Fracture surfaces of the tensile specimens at (a) (b) room temperature (c) (d) 750°C (e) (f) 850°C (g) (h) 950°C (see online version for colours)

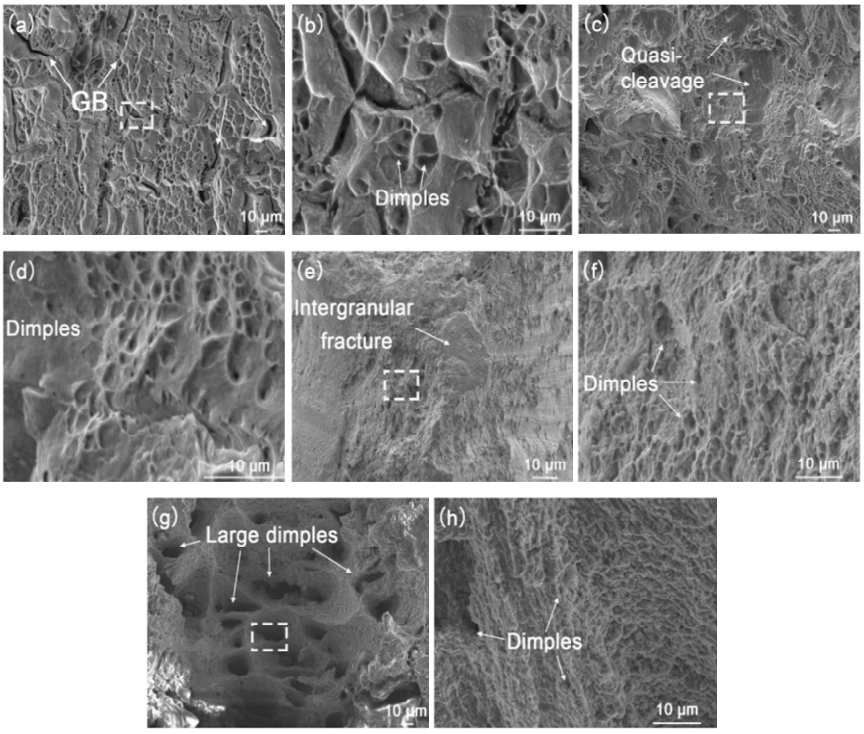

Source: Sun et al. (2019, p.107833)

The properties of weld joints are affected by the microstructure, especially mechanical properties (Zhang et al., 2014). The difference of microstructure phases is induced by the different thermal cycles. In UHPL welding, the cooling rate is high, and the peak temperature of different parts is different greatly. A high cooling rate facilitates obtaining grains with high hardness and strength (Hu et al., 2009; Wang et al., 2013; Atabaki et al., 2016), which will improve the strength and hardness of welds (Li et al., 2015a; Chen et al., 2017a), but reduce the impact performance (Wu et al., 2018; Yang et al., 2010a). According to fracture surfaces of the tensile specimens (Figure 3) (Sun et al., 2019), the fracture mode is ductile rupture both at room and high temperature, and better plasticity at high temperature than at room temperature. The exception to all this: for martensitic steel, the impact toughness is increased by the secondary-tempering phase in heat-affected zone (HAZ) (Wu et al., 2018). In addition, the dendritic segregation is often introduced by a high cooling rate (Ren et al., 2015), which affects the uniformity of weld microstructure and properties, and deteriorates the weld properties. Meanwhile, the high-

gradient thermal cycling at different parts of weld joint results in a great difference in the mechanical properties between the weld and the base metal, which is an undesirable quality (Sokolov et al., 2011; Yang, 2016). Reducing welding speed or preheating decreases the difference between the weld and the base metal, and increases the stability of the process (Sokolov et al., 2011; Yang, 2016).

3 Weld defects in UHPL welding

Weld defects are mainly caused by the instability of welding process. Welding instability is significantly enhanced in the process of UHPL welding, thus weld defects generated during this process greatly limits weld joint performance. The investigations of weld defects in UHPL focuses on the welding of medium thickness plates. The common weld defects consist of the splash, surface collapse, bottom hump, incomplete welding, etc. as shown in Figure 4 (Chen et al., 2018a). In UHPL welding of stainless steel, underfilling and humping weld beads are formed under the conventionally and tightly focused conditions respectively at 100 mm/s or higher welding speeds (Kawahito et al., 2009). Investigating the formation mechanism and control methods of weld defects is important to guarantee the stability and reliability of the weld joint. The formation mechanism and the control methods of weld defects (splash, surface collapse, porosity, and bottom hump) are introduced and analysed in the following part.

Figure 4 Weld defects of UHPL welding, (a) splash (b) surface collapse and bottom hump (c) nail-head shaped weld (d) incomplete welding

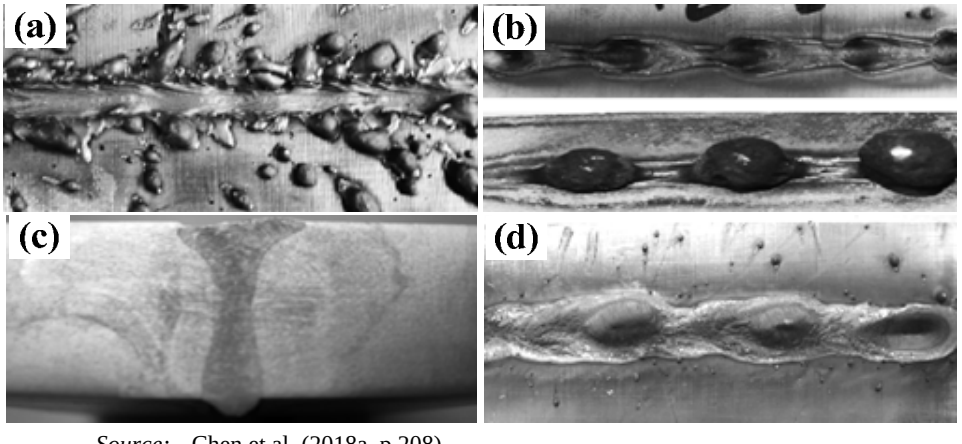

Source: Chen et al. (2018a, p.208)

The previously published work has shown that spatter behaviour is related to the violent evaporation of high temperature and liquid metal in UHPL welding (Kawahito et al., 2009; Fabbro, 2010; Kaplan et al., 2008; Cho and Na, 2007). A criterion of the spatter formation and eruption is that the local vertical momentum of the local melting metal exceeds the surface tension forces (Kaplan and Powell, 2011). The constriction and bulge formed on the rear keyhole wall is the key factor causing the vertical momentum of the melting metal, that is, the main reason for forming spatter (Ai et al., 2018). As shown in Figure 5, the formation mechanism of spatters on the upper and lower surfaces of the weld is deeply investigated by Zhang et al. (2013b) with different modes (low welding

speed, high welding speed, full penetration of melt, sporadic and continuous penetration of keyhole). Analysing from the formation mechanism of spatters, the side blowing gas jet assisted laser welding with a proper flow can be used to weaken spatters and restrain nail head weld (Xing et al., 2017; Chen et al., 2018a; Zhang et al., 2013b). A good weld with a little spatter and even without surface underfilling can also be acquired by appropriately tilting the incident direction of the laser beam (Li et al., 2014d) or directly blowing the protective gas to the centre of the keyhole (Zhang et al., 2009).

Figure 5 Behaviours of plasma, porosity, and weld pool when spatter is generated on the surfaces, (a) low welding speed on the upper surface (b) high welding speed on the upper surface (c) full penetration of melt on the lower surface (d) sporadic penetration of keyhole on the lower surface (e) continuous penetration of keyhole on the lower surface (see online version for colours)

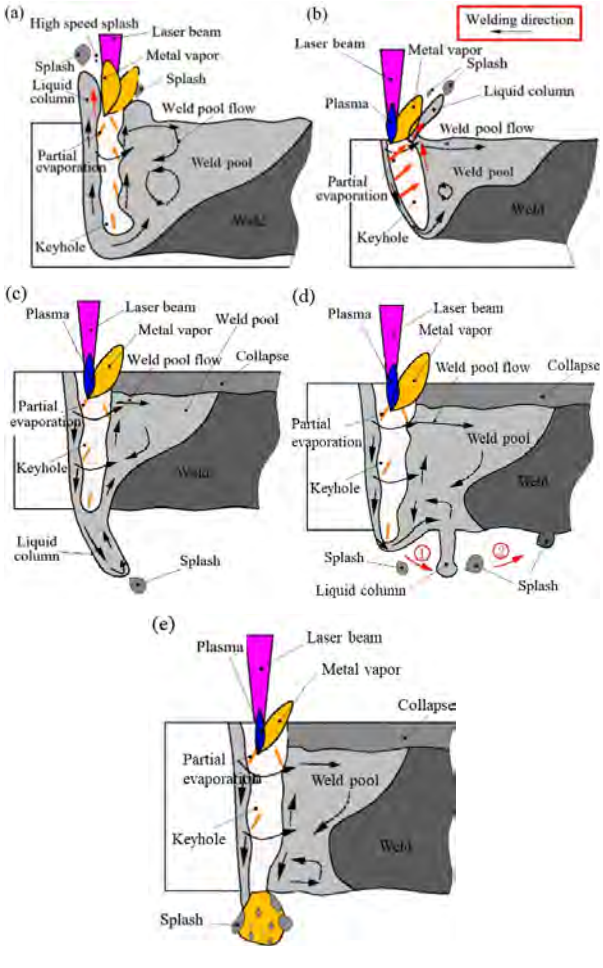

Source: Zhang et al. (2018, p.103)

The underfilling is often formed along the weld top surface concomitantly when the spatter is generated (Li et al., 2014b; Pan et al., 2016). For some kinds of metal with low melting temperature point and vaporisation temperature point, such as aluminium alloy,

magnesium alloy, etc. defects of underfilling and burn through are easily formed (Yang et al., 2010b). Instability of the keyhole and the weld pool is intensified, and the underfilling easily occurs, when the welding speed is too fast (Fabbro, 2010; Kawahito et al., 2007; Zhang et al., 2014). At full penetration of the keyhole, a deep underfill on the top surface of the weld and undercut on the bottom surface of the weld are formed owing to the massive direct melt loss from the weld pool (Zhang et al., 2018). The selected laser optical system with a long focus depth can be used to obtain full penetration welds without underfill defects (Matsumoto et al., 2017).

Figure 6 Transient formation process of periodic humps (see online version for colours)

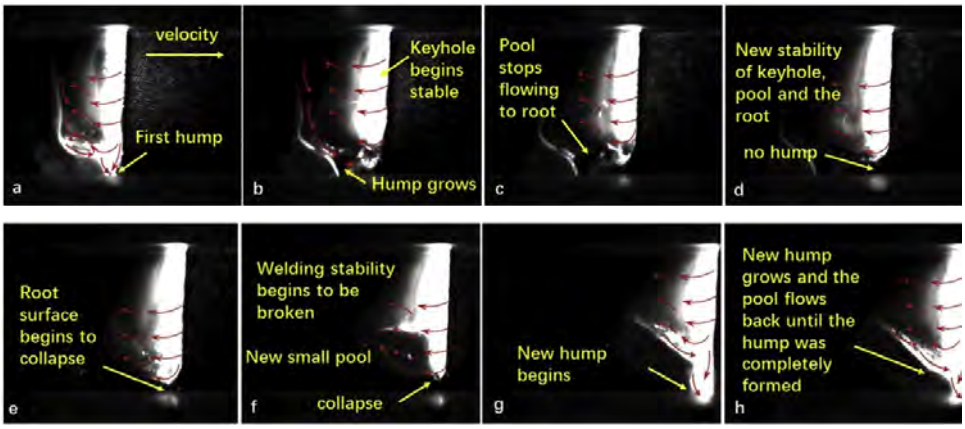

Source: Qi et al. (2019, p.116247-3)

The plasma evaporates violently at the tip of the keyhole in UHPL welding, many bubbles are forming at the bottom of the keyhole, which cannot be vented in time, leading to the formation of pores. The pulse-modulated laser with the trapezoidal waveform, 400–600 Hz frequency, and 30–50% duty cycle decreases the number and volume of pores in thick plates butt joints of AISI 321-AISI 405 stainless steel (Meng et al., 2019). Moreover, nitrogen shielding gas can be used to effectively suppress the porosity formation (Kawahito et al., 2009; Sun et al., 2017), but the suppression effects are greatly influenced by the base metal and welding wires (Seto et al., 2000). Using the wobble welding with appropriate parameters, a high-quality weld joint of 130 mm 5A06 aluminium alloy is obtained with average porosity of 1% and no other welding defects (Zou et al., 2019). For stainless steel with a thickness of 120 mm, the heat-conduction welding mode is useful to completely avoid the formation of pores (Wu et al., 2016).

Usually, a hump is easily formed on the collapsed root surface, especially for UHPL welding, when the bottom surface tension of the weld pool is not enough to offset the weight of the weld pool and compensate for the dynamic pressure of weld pool flow. The focal position is the most important welding parameter affecting hump formation (Zhang et al., 2019a). Positive defocus is more likely to produce large humps. The process of periodic humps is shown in Figure 6 (Qi et al., 2019). Increasing the bottom surface tension of the weld pool can compensate the gravity of the weld pool and suppress the hump. Blowing shielding gas on the weld bottom surface can suppress the weld pool collapse, reduce the occurrence of the hump, and improve the weld appearances due to the increasing surface tension energy of the weld pool (Zhang et al., 2014; Chen et al.,

2018a). Welding in the 2G position (laser beam perpendicular to the direction of gravity) or assisted by an external magnetic field can mitigate periodic root humps (Chen et al., 2018a; Qi et al., 2019; Guo et al., 2015; Jones et al., 2003). During narrow-gap laser wire filling welding of thick steel plates, the relative position between the laser beam and the filler wire has a great influence on the weld bead geometry and defects formation (Zhao et al., 2017).

4 Simulation and analysis in UHPL welding

The traditional experimental methods have the disadvantages of long period, and high cost regarding the welding process and weld defects in UHPL welding. Therefore, the simulations of keyhole and weld pool, residual stress, etc. are of great important in the research of UHPL welding process, defects, stress and deformation. The application of numerical simulation in UHPL welding is introduced and analysed from three aspects: the keyhole and weld pool simulation, the welding residual stress simulation, and the phase change process simulation.

The simulation of keyhole and weld pool better demonstrate the inner mechanism of weld formation and weld defects. The establishment of the self-consistent keyhole model breaks the previous assumption that the equilibrium radius of the keyhole is equal to the laser beam radius (Kroos et al., 1993). The equilibrium radius of the keyhole is larger. Ki et al. (2002) found that the effective laser absorptivity keeps fluctuating as a keyhole deepens (Mazumder et al., 2002; Ki et al., 2002). Even the stable keyhole has been formed, the shape of the keyhole is constantly fluctuating. Due to the different effects of convective heat transfer, the front wall tends to a large angle, while the back wall is steep (Kaplan, 1994). The front wall is inclined and stable, while the rear wall fluctuates due to insufficient energy absorption. The fluctuation of the rear wall and stability of keyhole can be improved by using an additional beam or an adequate intensity distribution irradiating this rear wall (Wang et al., 2010). And the amplitude of keyhole depth fluctuations can be significantly decreased by dual-beam laser welding under the same heat input condition (Figure 7) (Pang et al., 2015). In addition, Solana and Ocaña (1997) obtained accurate three-dimensional geometry of the keyhole and weld pool at medium welding speeds. The results of the study on the dimensions of the weld pool with a composite heat source show that the material conductivity is an important factor affecting the weld shape (Kazemi and Goldak, 2009).

Thick plate welding is an important application of UHPL welding. Compared with thin plates, the residual stress distribution of thick plate members is more complex, and the residual stress inside the thick plate is difficult to obtain. Not only the distribution of residual stress but also its distribution, reduction means, and possible defects are researched and predicted by utilising simulation. Yazdian et al. (2018) predicted residual stress fields and the distortion of thick welded plates of high-strength quenched and tempered steel. Furthermore, low thermal shrinkage induced by the hybrid laser/arc welding process was confirmed. Diao et al. (2019) simulated the residual stress to research the distribution law of welding residual stress in thick plates. In the thickness direction, the transverse residual stress and longitudinal residual stress are distributed symmetrically along the initial weld. Many factors influence the magnitude and distribution of residual stress. Studies have shown that double-sided welding can

effectively reduce angular deformation and the equivalent residual stress. The influence of external restraint on residual stress can be reduced by increasing workpiece width (Serizawa et al., 2011). The long weld has a smaller plastic strain, which can avoid weld crack (Serizawa et al., 2011). Welding residual stresses during thick plate welding can be reduced by adjusting reasonably the welding sequence (Figure 8) (Yang et al., 2019). Ibrahim et al. (2016) successfully predicted the crack initiation due to thermal stresses near the welds.

Figure 7 The calculated maximum keyhole depth evolutions during dual/single beam CO_2 laser welding

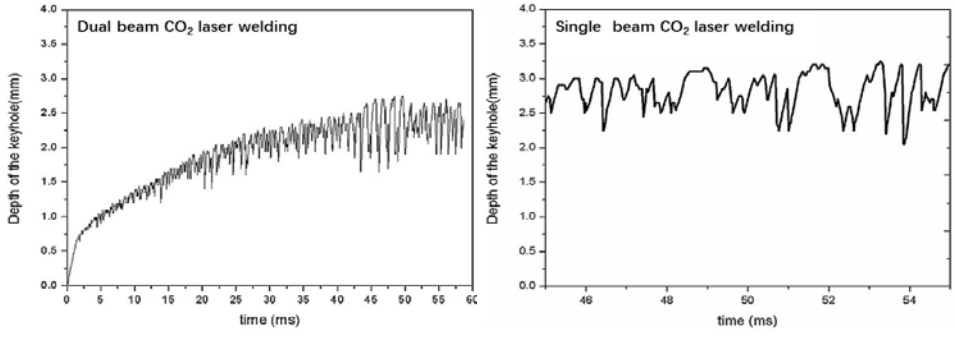

Source: Pang et al. (2015, p.138)

Figure 8 Contours of transverse and longitudinal stresses in different welding sequences (see online version for colours)

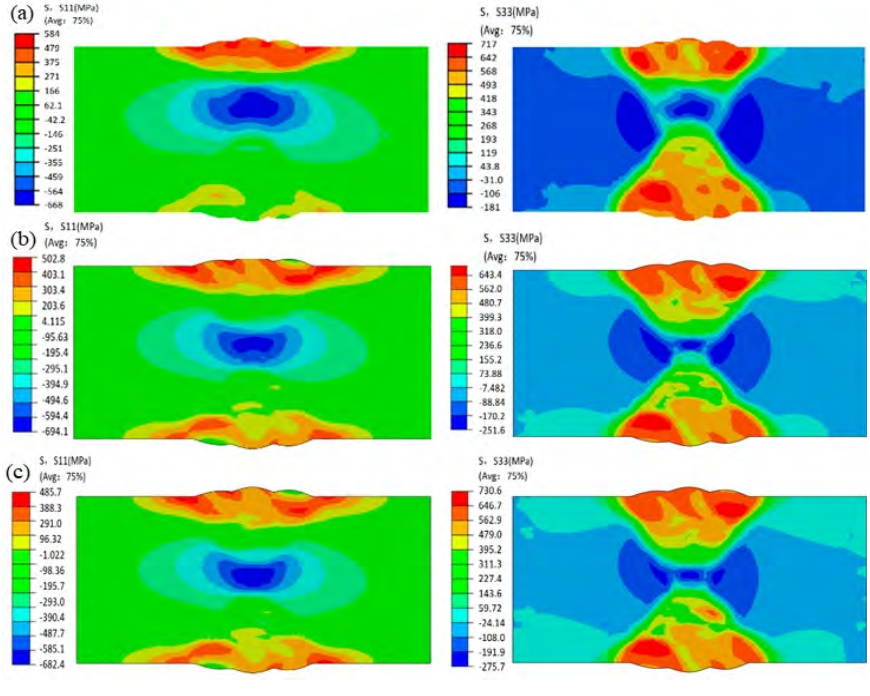

Source: Yang et al. (2019, p.2436-11)

The multiphase microstructure stress evolution plays an important role in revealing the formation mechanism of residual stress. The researches mainly include the study on the stress behaviour mechanism of the multiphase microstructure (Boyce et al., 2006; Zareie Rajani and Phillion, 2016) and the study on the influence of phase volume fraction on residual stress based on the macroscopic homogenisation of the multiphase microstructure (Liu et al., 2009; Mi et al., 2014). However, due to the high-temperature gradient of UHPL welding, the distribution of alloying elements and energy is uneven, which results in the poor consistency of elastic-plastic mechanical properties in the micro-zone of the weld. The microcosmic multiphase coordination mechanism and the macro set of residual stress need to be further studied.

Figure 9 (b) (d) (h) The predicted (a) (c) (e) (f) (g) Actual grain distribution and dendrite distribution (see online version for colours)

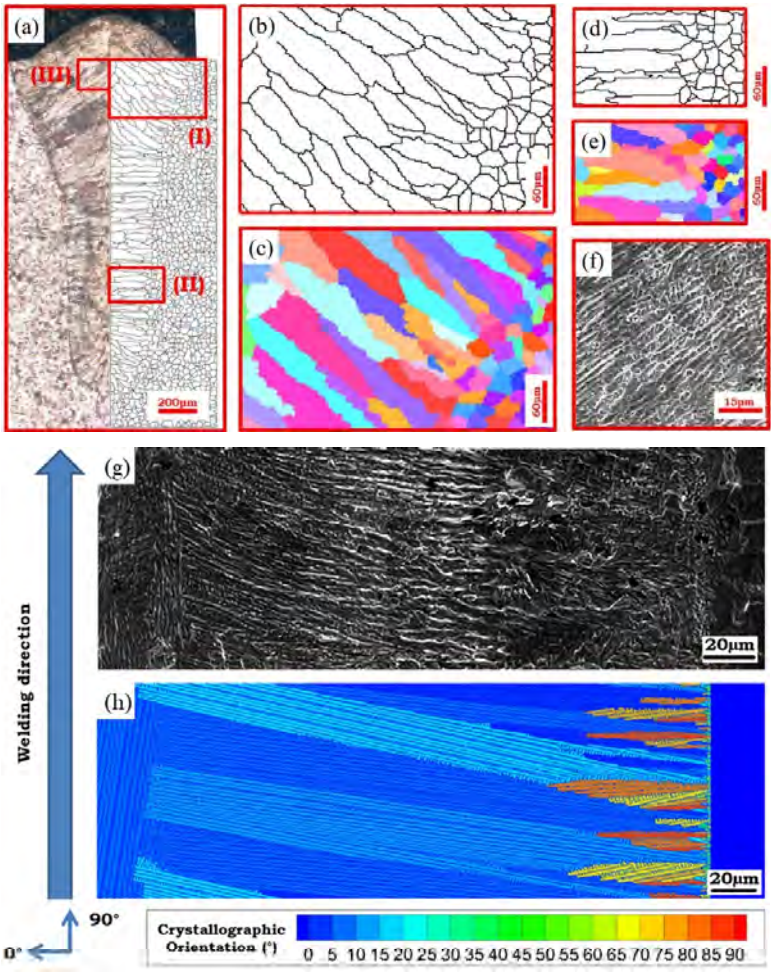

Source: Tan and Shin (2015, p.454)

Grain morphology and texture of welds significantly affect the properties of the corresponding joint. However, due to the opaqueness of metal, and the highly localised

and extremely fast solidification process, it is difficult to acquire the detailed dynamic evolution of solidification structures via experimental approaches. In recent research, three effective methods are developed to simulate the complicated solidification process in the weld pool, which included Monte Carlo (MC), phase field (PF), and cellular automaton (CA). MC method (Koseki et al., 2003) fully considers the randomness of microstructural evolution and can guarantee convergence. PH method (Zhan et al., 2009) has a clear physical basis, and the simulation process does not need to track complex interfaces. Cellular automata method (Wang et al., 2016; Tan and Shin, 2015) not only has a clear physical basis but also has randomness. Geng et al. (2019) developed a multi-scale model, combining the macro-scale model for heat transfer and fluid flow with the micro-scale phase-field model, to investigate the grain/sub-grain structure evolution in laser welding of 5083 aluminium alloy. Gao et al. (2021) calculated the grain growth and morphology evolution under different heat input conditions by the MC method. Tan and Shin (2015) inputted the generated thermal history of a macro-scale dynamic model into the cellular automata model (Figure 9), for the scale-span analysis of the grain growth and the dendrite morphology (Tan and Shin, 2015). Combining macro simulation with micro simulation for cross-scale analysis will greatly advance the mechanism research of weld formation and even the prediction of weld defects in UHPL welding. Kang et al. (2021) realised the evolution of porosity and grain coupling growth in the weld via a CA-finite element simulation method.

5 Field assisted laser welding

The field assisted welding is an effective method to improve welding stability and reduce weld defects. The effects of different external fields (external magnetic field, gravitational field, additional heat source, environmental pressure, and other external field) on the UHPL welding are reviewed.

External magnetic field can effectively improve the welding quality, stabilise the keyhole, inhibit the flow of the weld pool, improve the surface appearance and the weld profile, reduce the welding defects and optimise the weld performance (Vollertsen and Thomy, 2004; Avilov et al., 2012; Chen et al., 2016, 2017a, 2017b; Zhan et al., 2017). Especially, the weld root defects can be avoided by the external magnetic field in full penetration welding of the thick plate (Avilov et al., 2016). The dissipation effect of the magnetic field on the weld pool would not be influenced by the polarity (Bachmann et al., 2013). An optimal weld pool support can be obtained by numerical magnetic flux density (Bachmann et al., 2014). When the welding temperature exceeded the Curie temperature, a maximum inductive electromagnetic force would occur owing to the magnetic hysteresis effect (Qi and Chen, 2018). The application of steady electromagnetic force (SEMF) breaks this limitation. And the electromagnetic force can be adjusted by changing the current and the density of the magnetic field (Qi and Chen, 2018; Zhao et al., 2010). Moreover, a Lorentz force can be built by the magnetic field that is aligned perpendicular to the welding direction. Hereby, the flow of weld pool will be inhibited, resulting in the enhancement of welding process stability, and the spatter and melt ejections will be reduced (Bachmann et al., 2013). The Lorentz force can improve the element distribution over the entire thickness of the material as well as the mechanical properties (Shen et al., 2016). Li et al. (2021) introduced a new approach of electromagnetic assisted wire wobbling to regulate energy allocation, melt flow, and

metallurgical structure in laser welding of 316 L stainless steel. The electromagnetic assisted wire wobble laser welding can enhance the sidewall wetting and refine the grain.

Figure 10 A comparison of processing windows between 1G and 2G positions (see online version for colours)

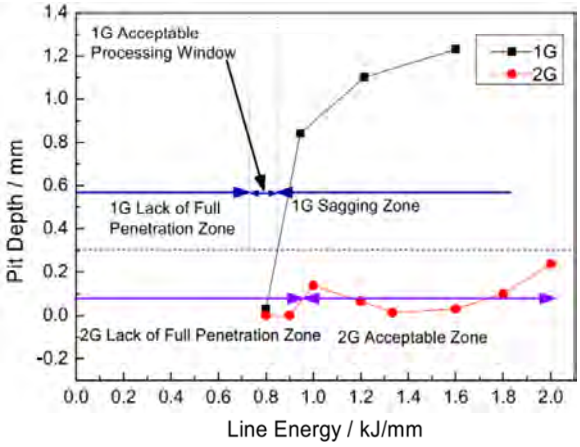

Source: Shen et al. (2016, p.022418-6)

Horizontal (2G) position welding is important to the manufacture of large and heavy structures, and in some cases, it is the only viable welding position. Comparing 1G welding position (laser directed towards the ground), welding in the 2G position (laser beam perpendicular to the direction of gravity) can mitigate some of the common welding defects including undercut and sagging (Guo et al., 2015). Meanwhile, the processing window of the 2G position is wider than that of the 1G position (Figure 10) (Shen et al., 2016). Maybe caused by the dumbbell shape (or X-shape) weld and relative wider weld, the pores of weld joints in the 2G position are relatively less.

The addition of other heat sources makes it possible to obtain a large penetration under a small laser power, which reduces the requirements of laser welding. The most common one is laser-arc hybrid welding. It improves the weld appearance, reduces the width of the HAZ, and eliminates or reduces the weld defects. Moreover, welding efficiency also can be improved, achieving the synergistic effect of 1 + 1 > 2. The arc-leading weld has a significant advantage in defect suppression, especially hump (Tang et al., 2019). Meanwhile, the distribution of hardness is more uniform and stable, and the impact toughness of weld is 21.89% higher than laser-leading manner. Single-sided welding of X70 pipeline steel plate with a thickness of 23 mm is realised by laser-double arc welding, which significantly reduces the welding time (Seffer et al., 2014).

In addition, using the combination of multiple laser heat sources has a similar effect as laser-arc hybrid welding. Through this technology, butt joint with 60 mm thickness is achieved, which improves the productivity by 3 to 4 times with a tremendous improvement of the deformation (Coste et al., 2003). Dual-beam laser welding is also considered in aircraft panel manufacturing, which can optimise the weld quality by improving the stability of the keyhole and weld pool (Pang et al., 2015; Ma et al., 2017; Li et al., 2018b).

Many researches indicate that reducing pressure is helpful to deepen the weld penetration (Katayama et al., 2001; Gao et al., 2017; Jiang et al., 2017; Börner et al., 2011; Blackburn et al., 2013; Punshon and Smith, 2013; Youhei et al., 2014). The effect of decompression on the weld penetration depth of different materials is different. The weld penetration depth of stainless steel increases with the decrease of environmental pressure (Youhei et al., 2014). By contrast, it is found that the weld penetration depth of aluminium can be increased by decreasing environmental pressure at pressures of 10 kPa or more. But the effect of reduced pressure on weld penetration depth is weak at pressures of 1 kPa or less. Besides, no matter what the material is when the ambient pressure was below 10 kPa, there is little change in the weld penetration (Wang et al., 2019). The influence of ambient pressure on the shape of weld bead was related to the welding speed (Börner et al., 2011). The lower the welding speed, the more significant the effect of ambient pressure on the weld penetration will be. When the welding speed was higher than 4 m/min, the ambient pressure has little influence on the weld penetration. Similar to traditional laser welding, there is an optimal defocus distance of laser welding under subatmospheric pressure (Jakobs and Reisgen, 2015). In addition, joint edge surface roughness and pre-set air gap also influence the weld quality and penetration depth in partial vacuum atmospheric conditions laser beam welding (Sokolov et al., 2015).

However, the test condition of decompression is very strict and the vacuum chamber of the corresponding size is needed, which is a major obstacle to thick plate laser welding featuring large components in the manufacturing fields of nuclear power, ships, and major equipment. Combined with the characteristics of vacuum welding, Tang et al. (Luo et al., 2016, 2014) propose a new method of mobile negative pressure laser welding, which provides a new way for welding and manufacturing thick plate components. The core structure of the new welding device is a negative pressure chamber (Figure 11).

Figure 11 Structure of improved local vacuum chamber (see online version for colours)

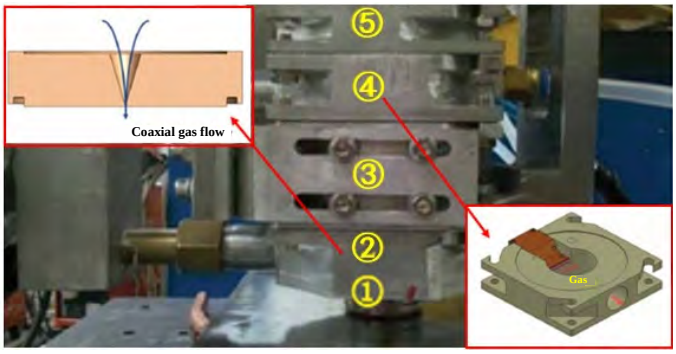

Notes: ① negative pressure module; ② tapered hole module; ③ fixed module; ④ air knife module; ⑤ the lens module.

Source: Luo et al. (2014, p.700)

Increasing environmental oxygen concentration has a positive impact on the deep penetration weld (Naito et al., 2006; Ribic et al., 2011). On the one hand, the laser absorption coefficient increases with the increase of environmental oxygen concentration (Zhao et al., 2010). On the other hand, carbon monoxide (CO) is formed at the keyhole

surface under the action of oxygen, and additional pressure from CO leads to an increase in penetration (Ribic et al., 2011). Adding appropriate activating fluxes can improve welding quality and increase welding depth without increasing input energy (Vidyarthy and Dwivedi, 2016; Ribic et al., 2011; Mishra et al., 2008; Wang et al., 2021; Ma et al., 2014). Adding sulphur powder increases molten metal fluidity, elongates weld pool, and promotes heat transmission during UHPL welding, which improves the weld depth (Li et al., 2017). Ultrasonic assisted laser welding can also effectively improve weld joint performance (Vorontsov et al., 2018; Liu et al., 2015; Li et al., 2016, 2018a), but it has not been used in UHPL welding.

6 Summary and future outlook

In this article, a detailed review of the research status on the UHPL welding processing is discussed from four aspects: processing stability, weld defects, numerical simulation, and field assisted welding. The stability of UHPL welding process is analysed from the morphological characteristics and dynamic behaviour of keyhole, weld pool, and plume, and the mechanical properties of weld joints. The formation mechanism and control methods of common weld defects are introduced and analysed. The application of numerical simulation in UHPL welding is introduced and analysed from three aspects: keyhole and weld pool simulation, welding residual stress simulation, and phase change process simulation. The effects of different external fields (external magnetic field, gravitational field, additional heat source, environmental pressure, and other external fields) on the UHPL welding are reviewed. The following conclusions are obtained.

1 Due to the increase of input laser energy, the intensified oscillation of keyhole, weld pool, and plume would increase the unstability of UHPL welding and deteriorate the properties of weld joints. It is of great significance to study the morphological characteristics and dynamic behaviour of keyhole, weld pool, and plume to improve the stability of UHPL welding. The observation methods of keyhole and weld pool are mainly divided into two types: one is that the material was welded to transparent glass and observed directly by a high-speed camera; one is using different elements for marking the melting metal. Both of these two types are used in keyhole observation, and weld pool observation mainly depends on the second type. Plume is studied by a high-speed camera and image processing. Their behaviours are periodic and interact with each other.

2 The formation mechanism and control methods of common weld defects are introduced and analysed, as follow:

3 Simulation calculation is an essential tool for optimising the quality of UHPL welding, because of detailed physical quantities analysis, short period, and low cost. It mainly includes the simulation of keyhole and weld pool, residual stress, etc. The simulation not only helps to explain the mechanism of weld formation and residual stress formation, but also can predict weld defects. But the microcosmic multiphase coordination mechanism and the macro set of residual stress need to be further studied. Although microstructure simulation is rarely used in UHPL welding, combining micro simulation with macro simulation for cross-scale analysis will greatly promote the mechanism research of weld formation and even the prediction

of weld defects in UHPL welding. In addition, the balance between accuracy and efficiency is always difficult, especially the simulation calculation of thick plate welding.

4 Based on pure laser welding, external field assistance such as magnetic field and gravity field is added to further optimise the weld performance. External magnetic field and welding in the 2G position (laser beam perpendicular to the direction of gravity) have a significant effect on the inhibition of hump. Laser welding adding other heat sources, such as laser-arc hybrid welding and multi-laser heat source, welding in partial vacuum atmospheric conditions, increasing environmental oxygen concentration, and adding appropriate activating fluxes are helpful to deepen the weld penetration. In addition, ultrasonic assisted laser welding can also effectively improve weld joint performance, but it has not been used in the field of thick plate welding. All in all, field assisted laser welding has great potential in UHPL welding, especially in the field of thick plate welding. However, the effect and mechanism of different fields on weld forming need more in-depth and multidisciplinary research.

Table 1 The formation mechanism and control methods of common weld defects

Type of weld defect	*Formation mechanism or main reasons*	*Control methods*
Spatter	With the violent evaporation of high temperature and liquid metal in UHPL welding, the rear keyhole wall constricts and bulges, the local vertical momentum of the local melting metal exceeds the surface tension forces, forming spatter.	The side blowing gas jet assisted laser welding with a proper flow; appropriately tilt the incident direction of the laser beam, or directly blow the protective gas to the centre of the keyhole.
Underfilling	The main reason is the material loss caused by metal vaporisation, formation of spatter and loss from the bottom of the weld pool, thus forming underfilling. It often occurs in some kinds of metal with low melting temperature points and vaporisation temperature points, such as aluminium alloy, magnesium alloy, and others.	Use the selected laser optical system with a long focus depth.
Pore	The plasma evaporates violently at the tip of the keyhole, many bubbles are forming at the bottom of the keyhole, which cannot be vented in time, leading to the formation of pores.	The pulse-modulated laser welding; nitrogen shielding gas; use the wobble welding with appropriate parameters; the heat-conduction welding mode.
Hump	When the bottom surface tension of the weld pool is not enough to offset the weight of the weld pool and compensate the dynamic pressure of weld pool flow, the weld bottom surface is easy to form humps. It is common in thick plate single pass welding because of the big weld pool.	Welding with negative defocus; blow shielding gas on the weld bottom surface; welding in the 2G position (laser beam perpendicular to the direction of gravity); welding assisted by an external magnetic field; the suitable relative position between the laser beam and the filler wire (in the narrow-gap laser wire filling welding).

The ultra-high-power laser welding, with obvious characteristics of fast welding speed, small heat input, small deformation, large aspect ratio, high alignment, and high directivity, has a huge application potential. Judging from the application of ultra-high-power laser in welding technology, ultra-narrow-gap single-pass and multi-pass laser welding of a large thick plate (Artinov et al., 2018), narrow-gap ultra-high-power laser-arc hybrid welding, and high-speed laser welding of an ultra-thin plate (Rong et al., 2022), are gradually becoming three important research interests.

There are three main problems with thick plate welding. First, the single-pass depth of fusion is limited by the laser power, and multiple passes are usually required, resulting in low welding efficiency. Second, for single-pass welding thick plate, it is difficult to overcome the welding defects, especially collapse and hump. Finally, for multi-pass welding thick plate, the shape and properties between layers are inhomogeneous, which has a great impact on the performance of welded joints. Narrow gap ultra-high-power laser-arc hybrid welding is an important way of joining thick plates. Not only a reasonable groove design is required, but also multi-pass laser-arc hybrid welding involves many process parameters, which is a complex manufacturing process. Moreover, with the further increase in the thickness of the plate, a series of insurmountable problems arise the transverse crack in the surfacing layer, porosity in bead edge, and non-fusion between layers (Lai et al., 2021). There are two main problems with high-speed laser welding of ultra-thin plates. First, precise calculation and control of the laser energy input are required, as much energy input will cause the join to fail. Second, deformation of the plate will be caused by the concentrated input of laser energy, so a suitable fixture is required. Further researches on the process stability of welding, weld defects, simulation, and field assisted welding are needed to improve these problems, thus promoting the application of UHPL welding in welding of large thick plate, laser-arc hybrid welding, and welding of ultra-thin plate.

Acknowledgements

This research is supported by the National Natural Science Foundation of China (51905191), the Major Project of Science and Technology Innovation Special for Hubei Province (2018AAA027), Wuhan Science and Technology Planning Project (201903070311520), and Postdoctoral Science Foundation of China (2021M691113).

References

Ai, Y., Jiang, P., Wang, C., Mi, G. and Geng, S. (2018) 'Experimental and numerical analysis of molten pool and keyhole profile during high-power deep-penetration laser welding', *International Journal of Heat and Mass Transfer*, Vol. 126, Part A, pp.779–789.

Ai, Y., Liu, X., Huang, Y. and Long, Y. (2021) 'Investigation of dissimilar fiber laser welding of low carbon steel and stainless steel by numerical simulation', *Journal of Laser Applications*, Vol. 33, No. 1, p.012046.

Artinov, A., Bachmann, M. and Rethmeier, M. (2018) 'Equivalent heat source approach in a 3D transient heat transfer simulation of full-penetration high power laser beam welding of thick metal plates', *International Journal of Heat and Mass Transfer*, July, Vol. 122, pp.1003–1013.

Atabaki, M.M., Yazdian, N., Ma, J. and Kovacevic, R. (2016) 'High power laser welding of thick steel plates in a horizontal butt joint configuration', *Optics and Laser Technology*, Vol. 83, No. 9, pp.1–12.

Avilov, V., Fritzsche, A., Bachmann, M., Gumenyuk, A. and Rethmeier, M. (2016) 'Full penetration laser beam welding of thick duplex steel plates with electromagnetic weld pool support', *Journal of Laser Applications*, Vol. 28, No. 2, p.22420.

Avilov, V.V., Gumenyuk, A., Lammers, M. and Rethmeier, M. (2012) 'PA position full penetration high power laser beam welding of up to 30 mm thick AlMg3 plates using electromagnetic weld pool support', *Science and technology of Welding and Joining*, Vol. 17, No. 2, pp.128–133.

Bachmann, M., Avilov, V., Gumenyuk, A. and Rethmeier, M. (2013) 'About the influence of a steady magnetic field on weld pool dynamics in partial penetration high power laser beam welding of thick aluminium parts', *International Journal of Heat and Mass Transfer*, Vol. 60, No. 1, pp.309–321.

Bachmann, M., Avilov, V., Gumenyuk, A. and Rethmeier, M. (2014) 'Experimental and numerical investigation of an electromagnetic weld pool support system for high power laser beam welding of austenitic stainless steel', *Journal of Materials Processing Technology*, Vol. 214, No. 3, pp.578–591.

Beyer, E., Bakowsky, L., Loosen, P., Poprawe, R. and Herziger, G. (1984) 'Development and optical absorption properties of a laser induced plasma during CO_2-laser processing', *Industrial Applications of High Power Lasers*, Vol. 455, No. 3, pp.75–80.

Blackburn, J., Allen, C., Smith, S., Punshon, C. and Hilton, P. (2013) 'Thick-section laser welding', *Proceedings of LAMP2013 – the 6th International Congress on Laser Advanced Materials Processing*, Niigata International Convention and Exhibition Center, Japan.

Börner, C., Dilger, K., Rominger, V., Harrer, T., Krüssel, T. and Löwer, T. (2011) 'Influence of ambient pressure on spattering and weld seam quality in laser beam welding with the solid-state laser', *ICALEO 2011: 30th International Congress on Laser Materials Processing, Laser Microprocessing and Nanomanufacturing*, Laser Institute of America, Vol. 621, No. 2011, pp.621–29.

Boyce, D.E., Dawson, P.R., Sidle, B. and Gnäupel-Herold, T. (2006) 'A multiscale methodology for deformation modeling applied to friction stir welded steel', *Computational Materials Science*, Vol. 38, No. 11, pp.158–175.

Bykovskiy, D.P., Petrovskii, V.N. and Uspenskiy, S.A. (2015) 'Investigation of the vapour-plasma plume in the welding of titanium by high-power ytterbium fibre laser radiation', *Quantum Electronics*, Vol. 45, No. 3, pp.218–223.

Chen, G., Chen, F., Zhou, C., Zhang, M., Zhong, P. and Mao, S. (2018a) 'Welding defect suppression of stainless steel thick plate joint by 10-kW level laser welding', *Applied Laser*, Vol. 38, No. 2, pp.207–214.

Chen, J., Wang, T., Gao, X. and Li, W. (2018b) 'Real-time monitoring of high-power disk laser welding based on support vector machine', *Computers in Industry*, April, Vol. 94, pp.75–81.

Chen, J., Wei, Y., Zhan, X. and Pan, P. (2017a) 'Weld profile, microstructure, and mechanical property of laser-welded butt joints of 5A06 Al alloy with static magnetic field support', *International Journal of Advanced Manufacturing Technology*, Vol. 92, Nos. 5–8, pp.1677–1686.

Chen, X., Pang, S., Shao, X., Wang, C., Xiao, J. and Jiang, P. (2017b) 'Three-dimensional transient thermoelectric currents in deep penetration laser welding of austenite stainless steel', *Optics and Lasers in Engineering*, April, Vol. 91, pp.196–205.

Chen, Y., Zhang, Y., Luo, Z., Han, S. and Vladyslav, K. (2017c) 'Microstructure and mechanical properties of TC4 titanium alloy medium plate joints welded by laser beam', *Applied Laser*, Vol. 37, No. 5, pp.662–667.

Chen, R., Wang, C., Jiang, P., Shao, X., Zhao, Z., Gao, Z. and Yue, C. (2016) 'Effect of axial magnetic field in the laser beam welding of stainless steel to aluminum alloy', *Materials and Design*, November, Vol. 109, pp.146–152.

Cho, J.H. and Na, S.J. (2007) 'Theoretical analysis of keyhole dynamics in polarized laser drilling', *Journal of Physics D: Applied Physics*, Vol. 40, No. 24, pp.7638–7647.

Coste, F., Janin, F., Hamadou, M. and Fabbro, R. (2003) 'Deep penetration laser welding with Nd: YAG lasers combination up to 11 kW laser power', *1st International Symposium on High-Power Laser Macroprocessing*, Osaka, Japan, Vol. 4831, pp.422–427.

Diao, L., Zhang, C., Chen, H. and Chen, J. (2019) 'Numerical simulation of narrow gap laser welding process of low alloy steel thick plate', *Hot Working Technology*, Vol. 48, No. 5, pp.199–202.

Fabbro, R. (2010) 'Melt pool and keyhole behaviour analysis for deep penetration laser welding', *Journal of Physics D: Applied Physics*, Vol. 43, No. 44, p.445501.

Fabbro, R., Slimani, S., Doudet, I., Coste, F. and Briand, F. (2006) 'Experimental study of the dynamical coupling between the induced vapour plume and the melt pool for Nd-Yag CW laser welding', *Journal of Physics D: Applied Physics*, Vol. 39, No. 2, pp.394–400.

Gao, M., Kawahito, Y. and Kajii, S. (2017) 'Observation and understanding in laser welding of pure titanium at subatmospheric pressure', *Optics Express*, Vol. 25, No. 12, pp.13539–13548.

Gao, Q., Jin, C. and Yang, Z. (2021) 'Morphology and texture characterization of grains in laser welding of aluminum alloys', *Welding in the World*, Vol. 65, No. 3, pp.475–483.

Geng, S., Ping, J., Guo, L., Gao, X. and Mi, G. (2019) 'Multi-scale simulation of grain/sub-grain structure evolution during solidification in laser welding of aluminum alloys', *International Journal of Heat and Mass Transfer*, March, Vol. 149, p.119252.

Guo, W., Liu, Q., Francis, J.A., Crowther, D., Thompson, A., Liu, Z. and Li, L. (2015) 'Comparison of laser welds in thick section S700 high-strength steel manufactured in flat (1G) and horizontal (2G) positions', *CIRP Annals – Manufacturing Technology*, Vol. 64, No. 1, pp.197–200.

Hu, L., Huang, J., Li, Z. and Wu, Y. (2009) 'Microstructure and properties of high power CO_2 laser welded pipeline steel', *Chinese Journal of Lasers*, Vol. 36, No. 12, pp.3174–3178.

Ibrahim, O.A., Lignos, D.G. and Rogers, C.A. (2016) 'Proposed modeling approach of welding procedures for heavy steel plates', *Engineering Structures*, November, Vol. 127, pp.18–30.

Ito, M., Yokozawa, F., Kawai, Y. and Tachibana, R. (1999) 'Welding characteristics of stainless steel in 10 kW laser beam welder', *ISIJ international*, Vol. 39, No. 7, pp.737–741.

Jakobs, S. and Reisgen, U. (2015) 'Laser beam welding under reduced pressure – range of possible applications for thick-plates', *Stahlbau*, Vol. 84, No. 9, pp.635–642.

Jiang, M., Tao, W., Wang, S., Li, L. and Chen, Y. (2017) 'Effect of ambient pressure on interaction between laser radiation and plasma plume in fiber laser welding', *Vacuum*, April, Vol. 138, pp.70–79.

Jones, L.P., Aubert, P., Avilov, V., Coste, F., Daenner, W., Jokinen, T., Nightingale, K.R. and Wykes, M. (2003) 'Towards advanced welding methods for the ITER vacuum vessel sectors', *Fusion Engineering and Design*, Vol. 69, Nos. 1–4, pp.215–220.

Kang, Y., Zhan, X., He, S., Liu, T. and Sun, L. (2021) 'Porosity-grain growth relationships in the laser beam deep penetration welding of 6061 aluminum alloy', *Journal of Adhesion Science and Technology*, Vol. 35, No. 13, pp.1372–1392.

Kaplan, A. (1994) 'A model of deep penetration laser welding based on calculation of the keyhole profile', *Journal of Physics D: Applied Physics*, Vol. 27, No. 9, pp.1805–1814.

Kaplan, A.F.H. and Powell, J. (2011) 'Spatter in laser welding', *Journal of Laser Applications*, Vol. 23, No. 3, p.32005.

Kaplan, A.F.H., Westin, E.M., Wiklund, G. and Norman, P. (2008) 'Imaging in cooperation with modeling of selected defect mechanisms during fiber laser welding of stainless steel', *ICALEO 2008: Proceedings of the International Congress on Applications of Lasers and Electro-Optics*, Temecula, USA, pp.789–798.

Katayama, S., Kobayashi, Y., Seto, N., Mizutani, M. and Matsunawa, A. (2001) 'Effect of vacuum on penetration and defects in laser welding', *Journal of Laser Applications*, Vol. 13, No. 5, pp.182–191.

Kawahito, Y., Matsumoto, N., Mizutani, M. and Katayama, S. (2008a) 'Characterisation of plasma induced during high power fibre laser welding of stainless steel', *Science and Technology of Welding and Joining*, Vol. 13, No. 8, pp.744–748.

Kawahito, Y., Kinoshita, K., Matsumoto, N., Mizutani, M. and Katayama, S. (2008b) 'Effect of weakly ionised plasma on penetration of stainless steel weld produced with ultra high power density fibre laser', *Science and Technology of Welding and Joining*, Vol. 13, No. 8, pp.749–753.

Kawahito, Y., Mizutani, M. and Katayama, S. (2007) 'Elucidation of high-power fibre laser welding phenomena of stainless steel and effect of factors on weld geometry', *Journal of Physics D: Applied Physics*, Vol. 40, No. 19, pp.5854–5859.

Kawahito, Y., Mizutani, M. and Katayama, S. (2009) 'High quality welding of stainless steel with 10 kW high power fibre laser', *Science and Technology of Welding and Joining*, Vol. 14, No. 4, pp.288–294.

Kawahito, Y., Wang, H., Katayama, S. and Sumimori, D. (2018) 'Ultra high power (100 kW) fiber laser welding of steel', *Optics letters*, Vol. 43, No. 19, pp.4667–4670.

Kazemi, K. and Goldak, J.A. (2009) 'Numerical simulation of laser full penetration welding', *Computational Materials Science*, Vol. 44, No. 3, pp.841–849.

Ki, H., Mohanty, P.S. and Mazumder, J. (2002) 'Modelling of laser keyhole welding: part II. Simulation of keyhole evolution, velocity, temperature profile, and experimental verification', *Metallurgical and Materials Transactions A: Physical Metallurgy and Materials Science*, Vol. 33, No. 6, pp.1831–1842.

Koseki, T., Inoue, H., Fukuda, Y. and Nogami, A. (2003) 'Numerical simulation of equiaxed grain formation in weld solidification', *Science and Technology of Advanced Materials*, Vol. 4, No. 3, pp.183–195.

Kroos, J., Gratzke, U. and Simon, G. (1993) 'Towards a self-consistent model of the keyhole in penetration laser beam welding', *Journal of Physics D: Applied Physics*, Vol. 26, No. 3, pp.474–480.

Lai, W., Ganguly, S. and Suder, W. (2021) 'Study of the effect of inter-pass temperature on weld overlap start-stop defects and mitigation by application of laser defocusing', *The International Journal of Advanced Manufacturing Technology*, Vol. 114, Nos. 1–2, pp.117–130.

Li, H., Hu, F., Cui, A., Dai, J., Huang, F. and Li, H. (2016) 'Effect of UPPLW on grain size of laser welding joints of TC4 titanium alloy', *Chinese Journal of Lasers*, Vol. 43, No. 8, pp.123–129.

Li, H., Hu, F., Cui, A., Dai, J., Huang, F. and Li, H. (2018a) 'Effect of ultrasonic vibration on microstructure and hardness of TC4 titanium alloy laser welding joints', *Rare Metal Materials and Engineering*, Vol. 47, No. 2, pp.624–629.

Li, L., Xia, H., Ma, G. and Peng, G. (2018b) 'Flow dynamics during single- and dual-spot laser welding with one common keyhole of 321 stainless steel', *Journal of Materials Processing Technology*, May, Vol. 255, pp.841–852.

Li, J., Liu, Y., Kang, K., Sun, Q., Jin, P., Liu, Y., Cai, C. and Sun, Q. (2021) 'A novel approach to regulate energy allocation and melt flow in narrow gap laser welding with electromagnetic assisted wire wobbling', *Journal of Materials Processing Tech.*, Vol. 47, No. 2, p.116909.

Li, S., Chen, G. and Zhou, C. (2015a) 'Effects of welding parameters on weld geometry during high-power laser welding of thick plate', *International Journal of Advanced Manufacturing Technology*, Vol. 79, Nos. 1–4, pp.177–182.

Li, Y., Feng, X., Zhang, D. and Cui, F. (2015b) 'High power fiber laser welding of lock butt joint of medium0Cr15Ni5Cu4Nb steel plate', *Transactions of the China Welding Institution*, Vol. 36, No. 7, pp.97–100.

Li, S., Chen, G., Zhang, M., Zhou, Y. and Zhang, Y. (2014a) 'Dynamic keyhole profile during high-power deep-penetration laser welding', *Journal of Materials Processing Technology*, Vol. 214, No. 3, pp.565–570.

Li, S., Chen, G., Katayama, S. and Zhang, Y. (2014b) 'Applied surface science relationship between spatter formation and dynamic molten pool during high-power deep-penetration laser welding', *Applied Surface Science*, June, Vol. 303, pp.481–488.

Li, S., Chen, G., Zhang, Y., Zhang, M., Zhou, Y. and Deng, H. (2014c) 'Investigation of keyhole plasma during 10 kW high power fiber laser welding', *Laser Physics*, Vol. 24, No. 10, pp.1–10.

Li, S.J., Chen, G.Y., Zhou, C., Chen, X.F. and Zhou, Y. (2014d) 'Plasma inside and outside keyhole during 10 kW level fiber laser welding', *Acta Physica Sinica*, Vol. 63, No. 10, pp.195–202.

Li, S., Deng, Z., Deng, H. and Xu, W. (2017) 'Microstructure and properties of weld joint during 10 kW laser welding with surface-active element sulfur', *Applied Surface Science*, December, Vol. 426, pp.704–713.

Liu, H.D., Hu, F.Y., Cui, A.Y. and Li, H.B. (2015) 'A study on the influence of ultrasonic processing on microstructure during laser welding phases', *4th Global Conference on Materials Science and Engineering (CMSE)*, Univ. Macau, Macau, China, Vol. 103, No. 1.

Liu, J., Lu, H. and Chen, J. (2009) 'Thermal-mechano-metallurgical coupled analysis of welding residual stress', *Transactions of the China Welding Institution*, Vol. 30, No. 2, pp.95–98.

Luo, Y., Tang, X. and Lu, F. (2014) 'Experimental study on deep penetrated laser welding under local subatmospheric pressure', *International Journal of Advanced Manufacturing Technology*, Vol. 73, Nos. 5–8, pp.699–706.

Luo, Y., Tang, X., Deng, S., Lu, F., Chen, Q. and Cui, H. (2016) 'Dynamic coupling between molten pool and metallic vapor ejection for fiber laser welding under subatmospheric pressure', *Journal of Materials Processing Technology*, March, Vol. 229, pp.431–438.

Ma, G., Li, L. and Chen, Y. (2017) 'Effects of beam configurations on wire melting and transfer behaviors in dual beam laser welding with filler wire', *Optics and Laser Technology*, Vol. 12, No. 91, pp.138–148.

Ma, L., Hu, S., Hu, B., Shen, J. and Wang, Y. (2014) 'Activating flux design for laser welding of ferritic stainless steel', *Transactions of Tianjin University*, Vol. 20, No. 6, pp.429–434.

Matsumoto, N., Kawahito, Y., Nishimoto, K. and Katayama, S. (2017) 'Effects of laser focusing properties on weldability in high-power fiber laser welding of thick high-strength steel plate', *Journal of Laser Applications*, Vol. 29, No. 1, p.12003.

Mazumder, J., Ki, H. and Mohanty, P.S. (2002) 'Role of recoil pressure, multiple reflections, and free surface evolution during laser keyhole welding', *International Congress on Applications of Lasers & Electro-Optics*, Laser Institute of America, Vol. 2002, No. 1, p.881291.

Meng, W., Xu, Z., Ma, Q., Yin, X. and Fang, J. (2019) 'Pulse fiber laser welding of AISI 321-AISI 405 stainless steel thick plates butt joints', *Journal of Materials Processing Technology*, Vol. 5, No. 271, pp.214–225.

Mi, G., Wei, Y., Zhan, X., Gu, C. and Yu, F. (2014) 'A coupled thermal and metallurgical model for welding simulation of Ti-6Al-4V alloy', *Journal of Materials Processing Technology*, Vol. 214, No. 11, pp.2434–2443.

Mishra, S., Lienert, T.J., Johnson, M.Q. and DebRoy, T. (2008) 'An experimental and theoretical study of gas tungsten arc welding of stainless steel plates with different sulfur concentrations', *Acta Materialia*, Vol. 56, No. 9, pp.2133–2146.

Naito, Y., Mizutani, M. and Katayama, S. (2006) 'Effect of oxygen in ambient atmosphere on penetration characteristics in single yttrium-aluminium-garnet laser and hybrid welding', *Journal of Laser Applications*, Vol. 18, No. 1, pp.21–27.

Pan, Q., Mizutani, M., Kawahito, Y. and Katayama, S. (2016) 'High power disk laser-metal active gas arc hybrid welding of thick high tensile strength steel plates', *Journal of Laser Applications*, Vol. 28, No. 1, p.12004.

Pang, S., Chen, W., Zhou, J. and Liao, D. (2015) 'Self-consistent modeling of keyhole and weld pool dynamics in tandem dual beam laser welding of aluminum alloy', *Journal of Materials Processing Technology*, March, Vol. 217, pp.131–143.

Penilla, E.H., Devia-Cruz, L.F., Wieg, A.T., Martinez-Torres, P. and Cuando-Espitia, N. (2019) 'Ultrafast laser welding of ceramics', *Science*, Vol. 365, No. 6455, pp.803–808.

Punshon, C. and Smith, S. (2013) 'Development of local vacuum technology for application of power beam welding to massive structures', *The Occasion of the 90th Year of General Relativity: Proceedings of the VII Asia-Pacific International Conference*, National Central University, Taiwan.

Qi, Y. and Chen, G. (2018) 'Root defects in full penetration laser welding of thick plates using steady electromagnetic force', *Journal of Materials Processing Technology*, Vol. 5, No. 260, pp.97–103.

Qi, Y., Chen, G., Deng, S. and Zhou, D. (2019) 'Periodic root humps in thick-plate laser welding using steady electromagnetic force', *Journal of Materials Processing Technology*, November, Vol. 273, p.116247.

Ren, W., Lu, F., Yang, R., Liu, X., Li, Z. and Elmi Hosseini, S.R. (2015) 'A comparative study on fiber laser and CO_2 laser welding of Inconel 617', *Materials and Design*, July, Vol. 76, pp.207–214.

Ribic, B., Tsukamoto, S., Rai, R. and DebRoy, T. (2011) 'Role of surface-active elements during keyhole-mode laser welding', *Journal of Physics D: Applied Physics*, Vol. 44, No. 48, p.485203.

Rong, Y., Wang, L., Wu, R. and Xu, J. (2022) [online] https://authors.elsevier.com/c/1diQ24bL22CDYI (accessed 7 September 2021).

Seffer, O., Lahdo, R., Springer, A. and Kaierle, S. (2014) 'Laser-GMA hybrid welding of API 5L X70 with 23 mm plate thickness using 16 kW disk laser and two GMA welding power sources', *Journal of Laser Applications*, Vol. 26, No. 4, p.42005.

Serizawa, H., Nakamura, S., Tanaka, M., Kawahito, Y., Tanigawa, H. and Katayama, S. (2011) 'Effect of mechanical restraint on weldability of reduced activation ferritic/martensitic steel thick plates', *Journal of Nuclear Materials*, Vol. 417, Nos. 1–3, pp.55–58.

Seto, N., Katayama, S. and Matsunawa, A. (2000) 'High-speed simultaneous observation of plasma and keyhole behavior during high power CO_2 laser welding-effect of shielding gas on porosity formation', *Journal of Laser Applications*, Vol. 12, No. 6, pp.245–250.

Shen, X., Li, L., Guo, W., Teng, W. and He, W. (2016) 'Comparison of processing window and porosity distribution in laser welding of 10 mm thick 30CrMnSiA ultrahigh strength between flat (1G) and horizontal (2G) positions', *Journal of Laser Applications*, Vol. 28, No. 2, p.22418.

Sokolov, M., Salminen, A., Katayama, S. and Kawahito, Y. (2015) 'Reduced pressure laser welding of thick section structural steel', *Journal of Materials Processing Technology*, May, Vol. 219, pp.278–285.

Sokolov, M., Salminen, A., Kuznetsov, M. and Tsibulskiy, I. (2011) 'Laser welding and weld hardness analysis of thick section S355 structural steel', *Materials and Design*, Vol. 32, No. 10, pp.5127–5131.

Solana, P. and Ocaña, J.L. (1997) 'A mathematical model for penetration laser welding as a free-boundary problem', *Journal of Physics D: Applied Physics*, Vol. 30, No. 9, pp.1300–1313.

Sun, J., Feng, K., Zhang, K., Guo, B., Jiang, E., Nie, P., Huang, J. and Li, Z. (2017) 'Fiber laser welding of thick AISI 304 plate in a horizontal (2G) butt joint configuration', *Materials and Design*, March, Vol. 118, pp.53–65.

Sun, J., Ren, W., Nie, P., Huang, J., Zhang, K. and Li, Z. (2019) 'Study on the weldability, microstructure and mechanical properties of thick Inconel 617 plate using narrow gap laser welding method', *Materials and Design*, August, Vol. 175, p.107823.

Tan, W. and Shin, Y.C. (2015) 'Multi-scale modeling of solidification and microstructure development in laser keyhole welding process for austenitic stainless steel', *Computational Materials Science*, February, Vol. 98, pp.446–458.

Tang, G., Zhao, X., Li, R., Liang, Y., Jiang, Y. and Chen, H. (2019) 'Microstructure and properties of laser-arc hybrid welding thick bainitic steel joints with different arc position', *Materials Research Express*, Vol. 6, No. 7, p.076547.

Ustundag, O., Bakir, N., Gumenyuk, A. and Rethmeier, M. (2021) 'Influence of oscillating magnetic field on the keyhole stability in deep penetration laser beam welding', *Optic and Laser Technology*, March, Vol. 135, p.106715.

Vidyarthy, R.S. and Dwivedi, D.K. (2016) 'Activating flux tungsten inert gas welding for enhanced weld penetration', *Journal of Manufacturing Processes*, April, Vol. 22, pp.211–228.

Vollertsen, F. and Thomy, C. (2004) 'Magnetic stirring during laser welding of aluminium', *International Congress on Applications of Lasers & Electro-Optics*, Laser Institute of America, Vol. 2004, No. 1, p.203.

Vorontsov, A.V., Dmitriev, A.V. and Beloborodov, V.A. (2018) 'Ultrasonic-assisted laser welding on ferrite-pearlite 09G2S (ASTM A516) steel', *AIP Conference Proceedings*, AIP Publishing LLC, Vol. 2051, No. 1, p.20324.

Wang, B., Zhao, Y. and Huang, J. (2013) 'Investigation on microstructure of thick plate stainless steel joint welded by multi-pass laser welding with filler wire', *Chinese Journal of Lasers*, Vol. 40, No. 2, pp.122–126.

Wang, C., Mi, G. and Zhang, X. (2021) 'Welding stability and fatigue performance of laser welded low alloy high strength steel with 20 mm thickness', *Optics and Laser Technology*, July, Vol. 139, p.106941.

Wang, J., Peng, G., Li, L., Si, C., Meng, S. and Gong, J. (2019) '30 kW-level laser welding characteristics of 5A06 aluminum alloy thick plate under subatmospheric pressure', *Optics and Laser Technology*, Vol. 6, No. 119, p.105668.

Wang, J., Wang, C., Meng, X., Hu, X., Yu, Y. and Yu, S. (2012) 'Study on the periodic oscillation of plasma/vapour induced during high power fibre laser penetration welding', *Optics and Laser Technology*, Vol. 44, No. 1, pp.67–70.

Wang, L., Wei, Y., Zhan, X. and Yu, F. (2016) 'A phase field investigation of dendrite morphology and solute distributions under transient conditions in an Al-Cu welding molten pool', *Science and Technology of Welding and Joining*, Vol. 21, No. 6, pp.446–451.

Wang, R., Lei, Y. and Shi, Y. (2010) 'Keyhole modeling during laser deep penetration welding', *Applied Mechanics and Materials*, Vol. 1, Nos. 29–32, pp.252–257.

Wang, Y., Shi, Q. and Tsai, H.L. (2001) 'Modeling of the effects of surface-active elements on flow patterns and weld penetration', *Metallurgical and Materials Transactions B: Process Metallurgy and Materials Processing Science*, Vol. 32, No. 1, pp.145–161.

Wu, S., Zhang, J., Yang, J., Lu, J., Liao, H. and Wang, X. (2018) 'Investigation on microstructure and properties of narrow-gap laser welding on reduced activation ferritic/martensitic steel CLF-1 with a thickness of 35 mm', *Journal of Nuclear Materials*, May, Vol. 503, pp.66–74.

Wu, S.K., Zou, J.L., Xiao, R.S. and Zhang, G. W. (2016) 'Ultra-narrow-groove laser welding for heavy sections in ITER', *Welding Journal*, Vol. 8, No. 95, pp.300–308.

Xing, M., Li, Z., Sun, J. and Zhang, W. (2017) 'Effect of small diameter side-blown gas flow on fiber laser welding of medium and heavy plat', *Chinese Journal of Lasers*, Vol. 44, No. 3, pp.143–147.

Yang, C. (2016) 'Laser welding robot on thick plate and the weld hardness analysis', *Electric Welding Machine*, Vol. 46, No. 4, pp.101–104.

Yang, D., Hu, L., Huang, J. and Ni, H. (2010a) 'Multi-pass welding process and microstructure of shipbuilding e-class thick steels using CO_2 laser welding', *Hot Working Technology*, Vol. 39, No. 19, pp.152–155.

Yang, J., Gang, S., Li, X., Chen, L. and Xu, F. (2010b) 'Typical joint defects in laser welding of aluminium-lithium alloy', *Laser in Engineering*, Vol. 22, Nos. 5–6, pp.337–350.

Yang, X.Y., Yan, G.Z., Xiu, Y.F., Yang, Z.W., Wang, G., Liu, W., Li, S.H. and Jiang, W.C. (2019) 'Welding temperature distribution and residual stresses in thick welded plates of SA738Gr.B through experimental measurements and finite element analysis', *Materials*, Vol. 12, No. 15, p.2436.

Yazdian, N., Derakhshan, E.D. and Kovacevic, R. (2018) 'Numerical prediction and experimental analysis of the residual stress fields and generated distortion in hybrid laser/arc welded thick plates of high-strength steels', *International Journal of Advanced Manufacturing Technology*, Vol. 98, Nos. 9–12, pp.2725–2735.

Youhei, A., Yousuke, K., Hiroshi, N., Koji, N., Masami, M. and Seiji, K. (2014) 'Effect of reduced pressure atmosphere on weld geometry in partial penetration laser welding of stainless steel and aluminium alloy with high power and high brightness laser', *Science and Technology of Welding and Joining*, Vol. 19, No. 4, pp.324–332.

Zareie Rajani, H.R. and Phillion, A.B. (2016) '3-multi-scale modeling of deformation within the weld mushy zone', *Materials and Design*, March, Vol. 94, pp.536–545.

Zhan, X., Zhou, J., Sun, W., Chen, J. and Wei, Y. (2017) 'Effect of external applied steady magnetic field on the morphology of laser welding joint of 4-mm 2024 aluminum alloy', *Applied Physics A: Materials Science and Processing*, Vol. 13, No. 1, pp.1–10.

Zhan, X.H., Dong, Z.B., Wei, Y.H. and Ma, R. (2009) 'Simulation of grain morphologies and competitive growth in weld pool of Ni-Cr alloy', *Journal of Crystal Growth*, Vol. 311, Nos. 23–24, pp.4778–4783.

Zhang, D., Wang, M., Shu, C., Zhang, Y., Wu, D. and Ye, Y. (2019a) 'Dynamic keyhole behavior and keyhole instability in high power fiber laser welding of stainless steel', *Optics and Laser Technology*, June, Vol. 114, pp.1–9.

Zhang, Y., Zhang, N., You, D., Gao, X. and Katayama, S. (2019b) 'High-power disk laser welding statuses monitoring based on analyses of multiple-sensor signals', *Journal of Manufacturing Processes*, May, Vol. 41, pp.221–230.

Zhang, L., Zhang, G., Bai, X., Ning, J. and Zhang, X. (2016) 'Effect of the process parameters on the three-dimensional shape of molten pool during full-penetration laser welding process', *Journal of Advanced Manufacturing Technology*, Vol. 86, Nos. 5–8, pp.1273–1286.

Zhang, M., Chen, G., Zhou, Y. and Li, S. (2013a) 'Direct observation of keyhole characteristics in deep penetration laser welding with a 10 kW fiber laser', *Optics Express*, Vol. 21, No. 17, p.19997.

Zhang, M.J., Chen, G.Y., Zhou, Y., Li, S.C. and Deng, H. (2013b) 'Observation of spatter formation mechanisms in high-power fiber laser welding of thick plate', *Applied Surface Science*, September, Vol. 280, pp.868–875.

Zhang, M., Chen, G., Zhou, Y. and Liao, S. (2014) 'Optimization of deep penetration laser welding of thick stainless steel with a 10 kW fiber laser', *Materials and Design*, January, Vol. 53, pp.568–576.

Zhang, M., Zhang, Z., Tang, K., Mao, C., Hu, Y. and Chen, G. (2018) 'Analysis of mechanisms of underfill in full penetration laser welding of thick stainless steel with a 10 kW fiber laser', *Optics and Laser Technology*, January, Vol. 98, pp.97–105.

Zhang, X., Ashida, E., Katayama, S. and Mizutani, M. (2009) 'Deep penetration welding of thick section steels', *Materials Research*, Vol. 27, No. 2, pp.64–68.

Zhao, C.X., Kwakernaak, C., Pan, Y., Richardson, I.M., Saldi, Z., Kenjeres, S. and Kleijn, C.R. (2010) 'The effect of oxygen on transitional Marangoni flow in laser spot welding', *Acta Materialia*, Vol. 58, No. 19, pp.6345–6357.

Zhao, Y., Ma, S., Huang, J. and Wu, Y. (2017) 'Narrow-gap laser welding using filler wire of thick steel plates', *International Journal of Advanced Manufacturing Technology*, Vol. 93, Nos. 5–8, pp.2955–2962.

Zou, J., Li, L., Gong, J., Huang, R. and Li, Y. (2019) 'Aluminum alloy thick plate laser scanning wire filling welding porosity suppression', *Transactions of the China Welding Institution*, Vol. 40, No. 10, pp.43–47.